

## Pedestal instabilities during the L-H transition

F. Clairet<sup>1</sup>, A. Medvedeva<sup>2</sup>, G. D. Conway<sup>3</sup>, C. Bottereau<sup>1</sup> and ASDEX Upgrade Team

<sup>1</sup> CEA, IRFM, 13108 St. Paul-lez-Durance cedex, France.

<sup>2</sup> Aix-Marseille Université, CNRS, Centrale Marseille, M2P2 UMR 7340, Marseille, France.

<sup>3</sup> Max-Planck-Institut für Plasmaphysik, 85740 Garching, Germany.

### Introduction

High confinement regime (H-mode) [1] is a foreseen experimental condition for plasma fusion device as it provides the best confinement performances. On the other hand, the effects of deleterious ELM events on plasma facing components during this improved performance is a strong concern for future nuclear reactors. Since the discovery of the H-mode in ASDEX-Upgrade tokamak plasmas [2] the L-H transition is still an active subject of research. This transition occurs in a narrow region close to the edge and is characterized by a transport barrier, which leads to a steep pedestal pressure next to the separatrix in the confined plasma. In order to improve the overall knowledge of this transition we have used an ultra-fast continuous frequency swept reflectometry, which provides a high spatio-temporal resolution analysis of density, gradients and turbulence [3]. This work aims to characterize the evolution of the instabilities continuously from the I-phase generation to the ELM crashes.

### Diagnostic

Measurements were performed using V and W band X-mode reflectometry diagnostics installed on AUG. They can be frequency swept in 1  $\mu$ s with a dead time as short as 0.25  $\mu$ s in between sweeps which provides a sampling rate of 800 kHz. It allows the determination of the density and fluctuation profiles at the same time. While one sweep help to calculate a density profile, fixed frequency signals from sweep to sweep allows, as hoping system, to provide about 2000 probing frequency steps. The density fluctuations are determined from the analysis of the signal phase [4] as

$$\delta n/n \sim \sqrt{\nabla N_X^2} \cdot \delta \Phi_{rms}$$

where the phase fluctuations are calculated from the power spectrum  $P_{\delta\phi}(\omega) = |FFT(e^{i\delta\phi(t)})|^2$  where according the Parseval theorem  $\delta\Phi_{rms} = \sqrt{\int P_{\delta\phi}(\omega) d\omega}$  thus allowing a frequency selection of the turbulence.

### L-H transition

The edge transport barrier is the result of local and poloidally rotating flow induced by a radial electric field (whose origin is still not yet fully understood). This transition is accompanied by a reduction of the turbulence [5] due to a strong  $E_r \times B$  shear flow with the formation of a steep pedestal at the plasma edge because of an increase of the edge pressure gradient, which in turn

induces instabilities such ELMs. Before reaching the H-mode, an intermediate phase or I-phase establishes as a limit cycle oscillation (LCO) between L and H-mode confinement regimes.

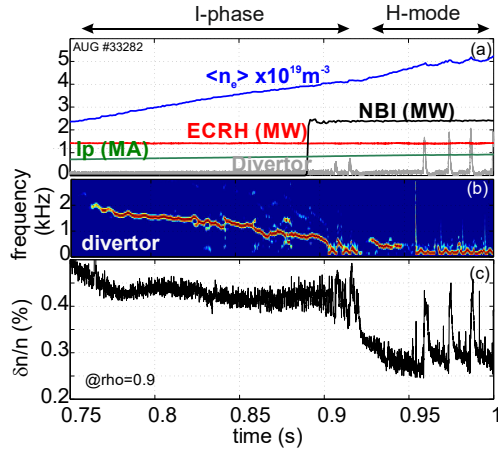


Figure 1 : (a) Experimental plasma conditions. (b) spectral analysis of the divertor shunt current signal to illustrate the LCO frequency during the I-phase. (c) density fluctuations.

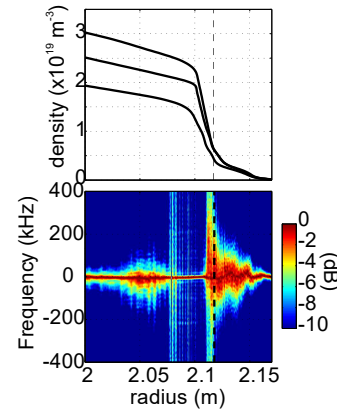


Figure 2 : Density profile steepening formation from L to H-mode with substantial and local modification of the turbulence spectral characteristics occurring in the pedestal.

## I-phase

We have made a comparative analysis between low and high frequency density fluctuations thanks to Parseval theorem described previously. The integration time to calculate the spectra (Fig. 3) is  $80 \mu\text{s}$  providing enough time resolution to resolve the I-phase oscillations, which is of the order of one kHz. As the global density fluctuations (the square represents the energy carried by the fluctuations) remains more or less constant during the I-phase regime we have observed (Fig. 4), by discriminating low ( $< 40 \text{ kHz}$ ) and high or broadband ( $> 40 \text{ kHz}$ ) frequencies, an opposite trend between both suggesting an energy transfer.

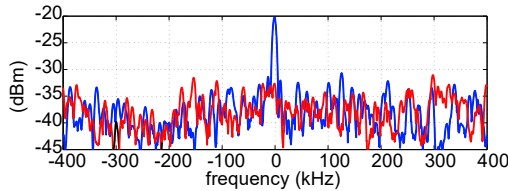


Figure 3 : Alternate frequency spectra during the I-phase.

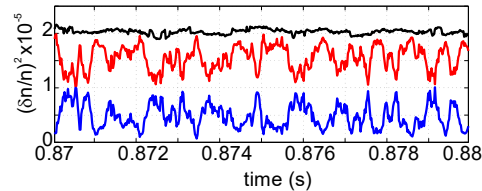
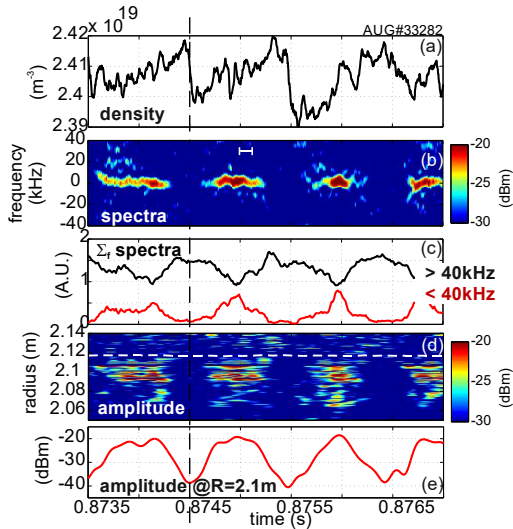


Figure 4 : Density fluctuations energy contained in the low frequency spectra ( $< 40 \text{ kHz}$ ) in blue and broadband frequencies ( $> 40 \text{ kHz}$ ) in red. In black is represented the fluctuations for all the frequency spectra.

The top pedestal density (Fig 5a) exhibits a sawtooth trend as an indication of an temporary improvement of the confinement. As the low frequency signal starts to show up (Fig. 5b and c) the density increases and when the broadband frequencies reach a certain level the pedestal relax. Moreover, when looking at the reflectometer signal (Fig. 5e and d), we notice a modulation of about 20 dB of the reflected amplitude with an increase when the low frequency

shows up and a decrease during the broadband spectra. A schematic of the process is drawn figure 6. This pattern of oscillations is compatible with a predator-prey-like flow-turbulence interaction model [6-8] and with the low frequency spectrum being the signature of the low frequency zonal flow.



→Figure 5 : (a) Top pedestal density. (b) Fluctuation spectra calculated with an integration time of 100  $\mu$ s (time resolution is represented by the white horizontal bar). (c) Amplitudes of the integrated spectra above and below 40 kHz. (d) Radial evolution of the reflected amplitude. (e) Amplitude variations of the reflected signal at R=2.1 m.

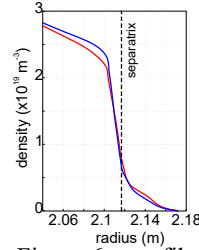


Figure 6 : profiles during the I-phase.

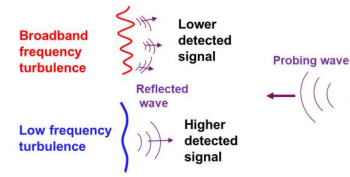
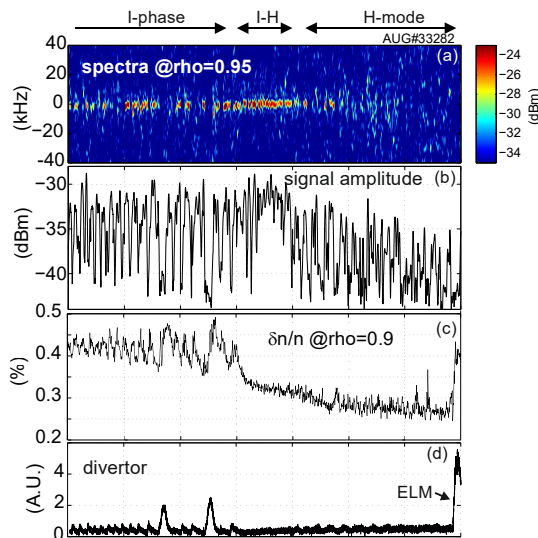


Figure 7 : Schematic of the plasma reflectivity efficiency according the turbulences.

### I-phase to established H-mode

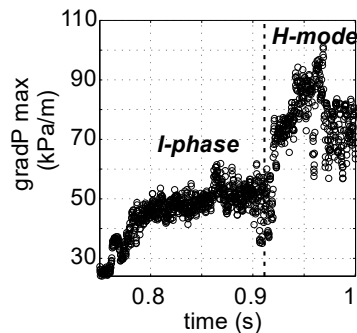
The I-phase appears to end at about  $t = 0.92$  s after two bigger bursts not always present in other discharges and not really clearly identified. Then, the low frequency turbulence amplitude is stabilizing up to about  $t = 0.93$  s as well as the amplitude of the reflected signal, which stops oscillating during the same period of time and the density fluctuations starts to decrease dramatically. From  $t = 0.93$  s the low frequency instability disappears totally and the signal amplitude, while still oscillating, steadily decreases up to the ELM event at  $t = 96$  s.



→Figure 8 : (a) Frequency spectra of the fluctuations exhibiting the evolution of the low frequency instability. (b) Amplitude of the reflected signal. (c) Density fluctuations. (d) Divertor shunt current.

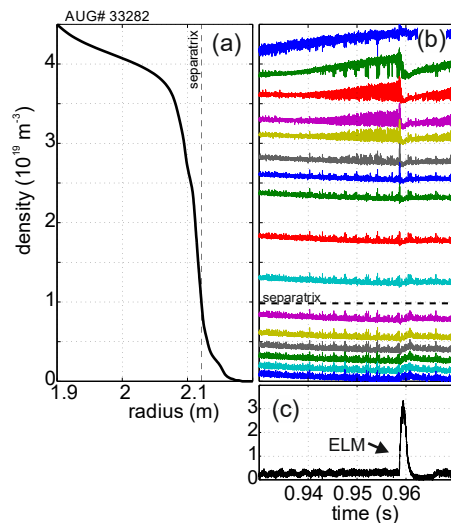
## ELM

As the plasma enters the H-mode, the pedestal pressure gradient increases substantially and the ELMs [9], most probably of type-I, are triggered.



→ Figure 9 : Evolution of the max pedestal pressure gradient during the L-I-H transition with an abrupt increase entering the H-mode

Before an ELM crash, a strong and fast density instability is recorded very locally on the top pedestal likely responsible of the amplitude loss observed figure 8b. This instability probably due to blob-filament activity [10] grows up to end with the ELM crash. In addition to this local perturbation, we measure fast and temporally more isolated density variations all along the pedestal. It is worth noting that during all these instabilities the confinement still improves as the core density keeps increasing and the density in the SOL decreases.



→ Figure 10 : (a) Average density profile just before the ELM. (b) Densities at fixed radii. (c) Divertor shunt current.

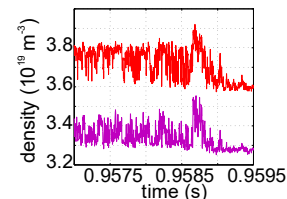


Figure 10 : Detail of the density instability recorded on the top pedestal..

## References

- [1] Wagner F. Plasma Phys. Control. Fusion **49**, B1 (2007)
- [2] Zohm H., Phys. Rev. Lett. **72**, 222 (1994)
- [3] Clairet F. et al. Rev. Sci. Instrum. **88**, 113506 (2017)
- [4] Mazzucato E. Rev. Sci. Instrum. **69**, 2201 (1998)
- [5] Moyer R.A. Physics of Plasmas **2**, 2397 (1995)
- [6] Kim E.J. et al Phys. Rev. Lett. **90**, 185006 (2003)
- [7] Conway G. D. et al. Phys. Rev. Lett. **106**, 065001 (2011)
- [8] Schmitz L. et al. Nucl. Fusion **57**, 025003 (2017)
- [9] Huysmans G.T.A. Plasma Phys. Control. Fusion **47** B165 (2005)
- [10] Kirk A. et al Plasma Phys. Control. Fusion **48** B433 (2006)